VERSITA

Central European Journal of **Chemistry**

A review on the synthesis of TiO$_2$ nanoparticles by solution route

Review Article

Shipra Mital Gupta*, Manoj Tripathi

*University School of Basic and Applied Sciences,
Guru Gobind Singh Indraprastha University. Delhi 110075, India*

Abstract: TiO$_2$ can be prepared in the form of powder, crystals, or thin films. Liquid-phase processing is one of the most convenient and utilized methods of synthesis. It has the advantage of allowing control over the stoichiometry, production of homogeneous materials, formation of complex shapes, and preparation of composite materials. However, there may be some disadvantages such as expensive precursors, long processing times, and the presence of carbon as an impurity. In comparison, the physical production techniques, although environment friendly, are limited by the size of the produced samples which is not sufficient for a large-scale production. The most commonly used solution routes in the synthesis of TiO$_2$ are reviewed.

Keywords: *Synthesis • Nanoparticles • TiO$_2$*
   © Versita Sp. z o.o.

1. Introduction

Fujishima and Honda [1] discovered the phenomenon of photocatalytic splitting of water over a TiO$_2$ electrode under ultraviolet light in 1972. Since then numerous promising energy and environmental applications in areas of photovoltaics, photocatalysis, photochromics and sensors have emerged [2-7]. Of the various semiconductors tested until date, TiO$_2$ is the most promising photocatalyst because of its appropriate electronic band structure, photostability, chemical inertness, and commercial availability. The effective utilization of clean, safe, and abundant solar energy through the TiO$_2$ photocatalysis provides promising solutions to the energy crisis and serious environmental challenges. TiO$_2$ has been widely used commercially in pigments [8], sunscreens [9,10], paints [11], toothpaste [12], *etc*. Various reports on the preparation, properties and applications of TiO$_2$ are available. In this review article, the most commonly used solution routes in the synthesis of TiO$_2$ are presented below.

2. Sol-gel technique

The sol-gel method is based on inorganic polymerization reactions. It includes four steps: hydrolysis, polycondensation, drying and thermal decomposition.

Hydrolysis of the precursors of the metal or non-metal alkoxides takes place with water or alcohols.

$$Ti(OR)_4 + 4H_2O \longrightarrow Ti(OH)_4 + 4ROH \text{ (hydrolysis)}$$
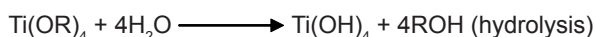
Where R = alkyl group

In addition to water and alcohol, an acid or a base also helps in the hydrolysis of the precursor. After condensation of the solution to a gel, the solvent is removed.

$$Ti(OH)_4 \longrightarrow TiO_2 + 2H_2O \text{ (condensation)}$$
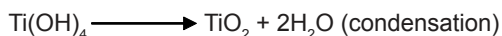
Calcination at higher temperature is needed to decompose the organic precursor. The schematic of the preparation process has been shown in Fig. 1 [13]. The size of the sol particles depends on the solution composition, pH and temperature. By controlling these factors, one can tune the size of the particles [14]. The major advantages of sol-gel processing for optical and electronic applications are: (i) ambient temperature of sol preparation and gel processing; (ii) product homogeneity; (iii) low temperature of sintering; (iv) ease of making multi-component materials and (v) good control over powder particle size and shape as well as size distribution [15].
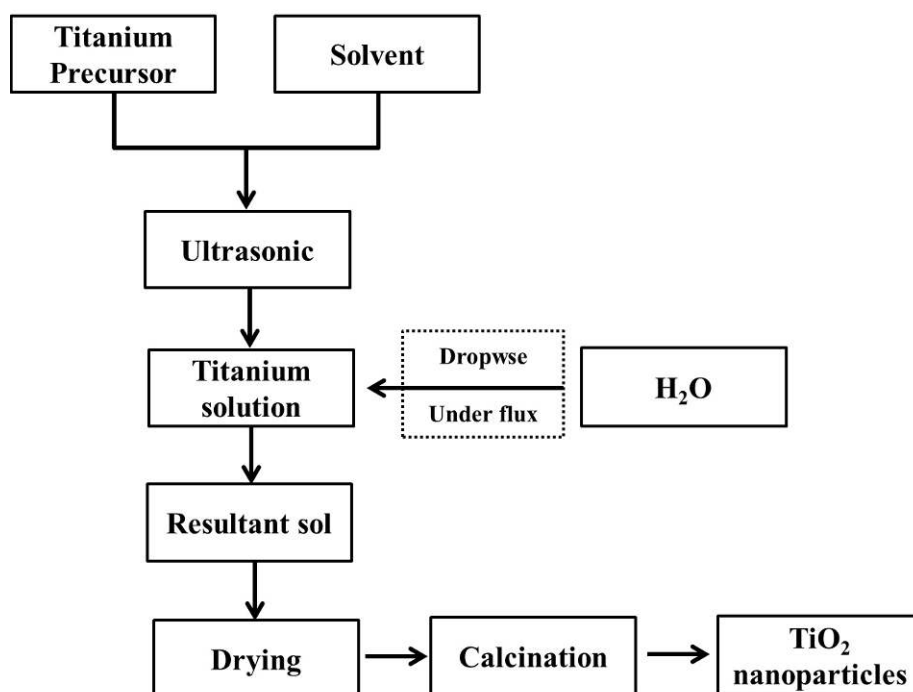
* E-mail: shipra.mital@gmail.com

Springer

Figure 1. Scheme of the preparation of TiO$_2$ nanoparticles sol-gel [13].

Nanostructures of TiO$_2$ have been synthesized with the sol-gel technique [16-21]. Mesoporous TiO$_2$ synthesized by the sol-gel method can be used as a ceramic membrane top layer [22,23] adsorbent [24] and catalyst support [25,26]. Solution sol-gel processing of titanium alkoxides and supercritical drying techniques have been used to prepare TiO$_2$ aerogels with much higher specific surface areas and tailored pore-size distributions [27,28]. Heller and co-workers [29-31], and others [32-34], have developed several methods for the creation of such films, *via* a sol-gel process. In their method, a titanium alkoxide (*e.g.* titanium isopropoxide) is hydrolyzed, coated onto a glass substrate, previously treated with sulphuric acid to produce a sodium-depleted layer, and calcined at a high temperature (usually 500°C) for a short time (approximately 20 min) [31]. Such films usually comprise anatase TiO$_2$ crystallites of 3-6 nm in diameter and therefore are transparent. Layers of TiO$_2$ can be built up using the sol-gel procedure to produce films approximately 60-100 nm thick which are not abraded when scribed with pencils of hardness H2 or softer and cannot be removed using Scotch Tape or rubbing with paper towels. Chau *et al*. [35] prepared well-dispersed surface-modified TiO$_2$ nanoparticles by a modified sol-gel process and incorporated them into epoxy matrix to form hybrid nanocomposites with higher refractive index than pure epoxy system. The TiO$_2$ solid content in the epoxy matrix could be more than 70 wt. percentage without affecting the optical transparency of the hybrid film. Loryuenyong *et al*. [36] prepared TiO$_2$ nanoparticles by a sol-gel process, employing titanium(IV) tetraisopropoxide as a starting precursor and ethanol/ isopropanol as an alcoholic solvent. The synthesized mesoporous TiO$_2$ was calcined at 300–700°C. It was found that pore collapsing, crystallite growth, and anatase-rutile phase transformation occurred with an increase in calcination temperatures. The use of isopropanol solvent was likely to inhibit the anatase–rutile transformation through the control of hydrolysis rate. The photocatalytic property of TiO$_2$ consisting predominantly of anatase crystallites improved the degradation of methylene blue under UVC light. Compared to ethanol, enhanced photocatalytic activity was obtained with isopropanol solvent through the thermal stability of anatase phase.

The sol-gel method is a versatile method for the synthesis of the doped nanomaterial with very high surface area to volume ratio. The incorporation of a metal ion in the sol during the gelation stage allows cations to be uniformly incorporated into the host lattice [37,38]. Thus, metal ions such as Ca^{2+}, Sr^{2+}, Ba^{2+} [39], Cu^{2+} [40,41], Fe^{3+} [42-46], V^{5+} [46,47], Cr^{3+} [46], Mn^{2+} [48,46], Pt^{4+} [49], Co^{2+} [50], Ni^{2+} [46], Pb^{2+} [51], W^{6+} [50], Zn^{2+} [44], Au^{3+} [52], Zr^{2+} [53], La^{3+} [54], Ag$^+$ [55,56] and Eu^{3+} [57] were introduced into TiO$_2$ powders and films by this method, and the photocatalytic activity was improved to varying extent. Wang *et al*. [58] have reported the preparation of Fe-doped TiO$_2$ to

obtain the uniform distribution of the dopant ions on TiO_2 particles by hydrolysis of a homogeneous mixture of organic titanium and organic iron precursors (Fe (III)-acetylacetonate) in isopropyl alcohol. Subasri et al. [59] synthesized plain and doped (Fe^{3+} and Nb^{5+}) TiO_2 by sol-gel route in combination with commercial nanoparticle dispersions and deposited them by dip coating on soda lime glass substrates. The doped TiO_2 films exhibited higher hydrophilicity than plain TiO_2 films in visible region. Photocatalytic activity for the degradation of methylene blue dye after 4 h exposure to sunlight was observed to be higher for doped TiO_2 coatings than that for the plain TiO_2 coating. Wang et al. [60] have synthesized a series of nitrogen-doped TiO_2 nanocatalysts by a two-step hydrolysis-calcination method. Pan et al. [61] prepared Cr-doped $TiO_{2-x}N_x$ powders by using sol-gel method and ammonia thermal treatment. Moon et al. [62] have reported TiO_2 modified with boron (B_2O_3/TiO_2) prepared by a sol-gel method which exhibited remarkable activity for the photocatalytic splitting of water. Song and Gao [63] reported polystyrene/SiO_2/TiO_2 multilayer hybrid spheres formed by a two-step sol-gel method. The polystyrene cores were removed by calcination in a furnace. Then, the final hollow SiO_2/TiO_2 double shell hybrid microspheres were obtained. The photocatalytic activity of hollow SiO_2/TiO_2 spheres with three layers of TiO_2 was slightly higher than that of Degussa P25, (commercially available TiO_2 powder sample) and the photocatalytic degradation of methylene blue by nitrogen-doped hollow hybrid sphere was about two times that of nitrogen-doped Degussa P25 powder.

In the last decade, various investigations have been carried out to produce nanotubes using sol-gel technique. Some researchers developed methods to deposit TiO_2 sol within the pores of template membrane (such as alumina membrane) to produce TiO_2 tubes, but the tube diameter is larger (ca. 200 nm). Cozzoli et al. [64-68] have reported the growth of high-aspect-ratio anatase TiO_2 nanorods by controlling the hydrolysis process of titanium tetraisopropoxide in oleic acid. Venkataramanan et al. [69] used ionic liquid $Ti(tOBu)_4$ as solvent in a surface sol-gel process to form TiO_2-coated cellulose fibres, which were removed during calcinations, yielding anatase TiO_2 nanotubes with morphologies of the cellulose fibres. Liu and He [70] produced nanoporous TiO_2 filaments with nanoporous platelets on the surface by mineralizing human hair via a surface sol-gel process. The TiO_2 microtubes inherited morphology of the hair template and displayed a tube-wall thickness that was tuneable by the number of sol-gel cycles. Pores in the microtubes were utilized as nanoreaction vessels for in-situ synthesis

of nanoparticles. Gu et al. [71] fabricated nanotube/hollow sphere hybrid structured functional anatase TiO_2 by surface sol-gel process using commercial filter paper as nanotube template and silica/polystyrene colloidal microspheres as hollow sphere templates. The microsphere and cellulose templates were removed by calcination / alkali treatment. The obtained anatase TiO_2 nanotubes were decorated with nanoscale TiO_2 hollow spheres with wall thickness of about 7.5 nm. The as-synthesized hybrid materials exhibited similar but superior photocatalytic efficiency compared with simple TiO_2 nanotube structured materials due to the higher surface area endowed by the complex highly porous structure. Zhang et al. [72] used bacterial cellulose membranes as the template to produce mesoporous TiO_2 networks consisting of interconnected anatase nanowires via a sol-gel process.

3. Microemulsion technique

Microemulsion may be defined as thermodynamically stable, optically isotropic solution of two immiscible liquids consisting of microdomains of one or both liquids stabilized by an interfacial film of surfactant [73]. It provides a micro-heterogeneous medium for the generation of nanoparticles. The formation of particles in such systems is controlled by the reactant distribution in the droplets and by the dynamics of inter-droplet exchange of reactants. The surfactant-stabilized microcavities provide a cage-like effect that limits particle nucleation, growth and agglomeration [74]. It occurs in two forms: O/W (oil in water) and W/O (water in oil) which are analogous to aqueous and non-aqueous mediums, respectively. The micelles are formed in aqueous medium, where the hydrophobic hydrocarbon chains of the surfactants are oriented toward the interior of the micelle, and the hydrophilic groups of the surfactants are in contact with the surrounding aqueous medium. On the other hand, reverse micelles are formed in non-aqueous medium where the hydrophilic head-groups are directed toward the core of the micelles, and the hydrophobic groups are directed outward [75]. The stability of the emulsions depends on the particle size, particle-particle interaction, particle-water interaction and particle-oil interaction [76,77]. The advantage with the microemulsion route is that the size of the particles can be affected by the ratio of surfactant to water [78]. The size of the produced particles is approximately the same as that of the water droplet in the reverse microemulsion [79]. Despite promising early studies, there have been only few reports of controlled TiO_2 synthesis from these microemulsions

[80,81]. In particular, hydrolysis of titanium alkoxides in microemulsion based sol-gel methods resulted in uncontrolled aggregation and flocculation [82,83] except at very low concentrations [73,84].

Deorsola *et al.* [85] adopted water-in-oil microemulsions to produce ultrafine and nanometric particles. The synthesis of TiO$_2$ nanoparticles has been carried out from a TiCl$_4$ solution emulsified into the oil phase (Fig. 2). Precipitation of spherical and ultrafine particles occurred due to the high instability of Ti precursor and the interaction among nanodroplets. Chhabra *et al.* [73] presented a microemulsion-mediated process for the synthesis of ultrafine nanoparticles of TiO$_2$. In their reported work, the aqueous microdroplets of water-in-oil microemulsions have been used as microreactors to precipitate the precursor hydroxide of titanium(IV). These precursor particles have been calcined at different temperatures to produce ultrafine TiO$_2$ particles. They observed that as calcination temperature decreases, the surface area of the particles decreases, and therefore, the particle size increases. The attenuation of ultraviolet radiation increases as the size of the TiO$_2$ particles decreases. They reported that only the anatase TiO$_2$ particles act as photocatalyst for photodegradation of phenol and the rutile form is inactive for this reaction. Wu *et al.* [86] showed that nanoparticles of both anatase and rutile type TiO$_2$ can be prepared at 120°C by hydrothermal treatment of microemulsions. The outcomes of their synthesis were of great interest because they yield the two TiO$_2$ polymorphs using the same temperature method. Gao *et al.* [87] reported the key steps for controlling the diameter of nano-TiO$_2$ in a W/O microemulsion reactor by the separation of the nucleation stage from the crystal growth stage. They used water droplet in a reverse micro-emulsion system as reactors to control the crystal growth of particles of similar size. Recently, Zubieta *et al.* [88] reported TiO$_2$ particles synthesized from an Aerosol OT/hexane/water reverse microemulsion system to evaluate the elimination of methylene blue dye. The crystalline composition, size of particles and their porosity were affected by the water content in the reverse micelles. Methylene blue photodegradation activity increased with an increase in the content of anatase phase and was not related with the specific area and particle size.

Cong *et al.* [89] synthesized nitrogen-doped nanocrystalline TiO$_2$ by microemulsion-hydrothermal process under nitric or hydrochloric acid environment. This did not require high calcination temperature and thus averted the agglomeration and sintering of the TiO$_2$ particles. The photocatalytic activity for the decomposition of rhodamine B by TiO$_2$ was greatly improved as compared with the undoped samples under visible light irradiation. Adán *et al.* [90] prepared a series of nanosized iron-doped anatase TiO$_2$ catalysts with different iron content (between 0.4 and 5.1 wt.%) by microemulsion method and examined their behaviour for UV photocatalytic degradation of aqueous phenol. An enhancement of the photocatalytic activity was observed for doping levels up to ca. 1 wt. percentage that was attributable to the effective introduction of Fe^{3+} cations into the anatase structure along with associated modifications of the surface acid/base properties. Zielińska *et al.* [91] obtained Ag-TiO$_2$ nanoparticles in the water-in-oil microemulsion system of water/AOT/cyclohexane. It was found that microemulsion method allowed obtaining Ag-TiO$_2$ nanoparticles with narrow particle size distribution regardless Ag content in the reaction system. The effect of Ag content used for preparation on the photocatalyst structure, surface area, crystallinity, and efficiency of removal of model organic compound and model microorganisms (E. *coli,* S. *aureus*, S. *cerevisiae*) from aqueous phase were systematically investigated. Their study suggested that silver-doped titanium dioxide nanoparticles can be used as effective growth inhibitor in various microorganisms.

4. Precipitation

The formation of the precipitate from a homogeneous liquid phase occurs because of physical transformation (change of temperature, pH, solvent evaporation, reactant concentration, *etc.*) or chemical process (addition of bases or acids, use of complex forming agents). In almost all cases, the formation of a new solid phase in a liquid medium results from two elementary processes which occur simultaneously or sequentially: (1) nucleation, *i.e.*, formation of the smallest elementary particles of the new phase which are stable under the precipitation conditions; and (2) growth or agglomeration of the particles [92]. The kinetics of nucleation and particle growth in homogeneous solutions can be adjusted by the controlled release of the anions and cations. Careful control of the kinetics of the precipitation can result in monodisperse nanoparticles. By controlling the factors that determine the precipitation process such as the pH, concentration of the reactants / ions, nanoparticles with narrow size distributions can be produced [14]. For the synthesis of oxides, co-precipitation process involves precipitation of hydroxides by the addition of a solution like NaOH, NH$_4$OH, urea, etc. to a raw material followed by heat treatment like calcination to crystallize the oxide [93]. Lower processing temperatures result in better metal dispersion than higher temperature treatments. This point is very important since a minimum particle
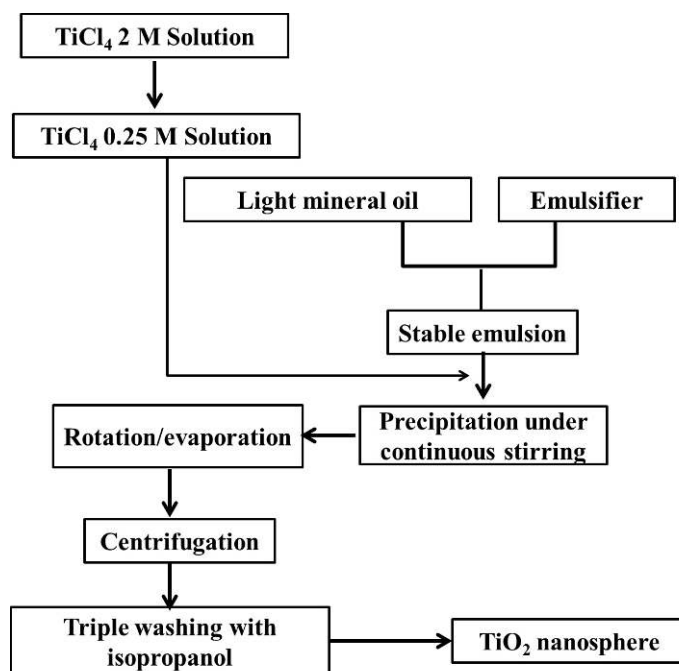
Figure 2. Scheme for the reactive microemulsion synthesis of TiO_2 nanopowders [85].

size is desired in order to achieve a maximum metal surface area per unit weight of metal [94]. In a system with two or more metallic compounds, the composition of the precipitate depends on the differences in solubility between the components and the chemistry occurring during precipitation. Generally, under the conditions of either a slow precipitation rate or poor mixing within the reaction medium, co-precipitation is selective and the co-precipitate is heterogeneous in composition. Subsequent to formation of the co-precipitate, hydrothermal treatments that transform amorphous precipitates to crystalline materials with improved thermal stability and surface acidity may be carried [95]. This procedure is widely applied to prepare molecular sieves [92]. One of the limitations of co-precipitation method is the tedious control of particle size and size distribution, as fast (uncontrolled) precipitation often causes formation of larger particles instead of nanoparticles [93].

Namin *et al.* [96] reported TiO_2 nanoparticles prepared by precipitation of aqueous $TiCl_4$ solution with ammonium hydroxide as precipitation agent. In their report, freshly prepared TiO_2 gel was allowed to crystallize under refluxing and stirring condition for 6 h over 90°C and oven dried over-night in temperature above 100°C. Shchipunov *et al.* [97] used ethylene glycol as the reaction media with dissolved polysaccharide xanthan which resulted in TiO_2 formation on the carbohydrate macromolecules like the biomineralization in living organisms. Polysaccharide in these syntheses served as a template. By varying the concentrations of xanthan

and water and also the synthesizing conditions, it was possible to manipulate the metal oxide morphology to fibrillar, particulate and plate-like structures. TiO_2 prepared at ambient conditions was amorphous. When it was calcined at temperatures between 300 and 900°C, crystalline anatase and rutile were found at 300 and 700°C, respectively.

Some groups of researchers have used chemical precipitation method for synthesizing doped-TiO_2 [98,99]. Sato *et al.* [100] reported nitrogen ion-doped TiO_2 nanoparticles obtained by the homogeneous precipitation in hexamethylenetetramine-titanium trichloride mixed solution followed by heat treatment in the solution at desired temperatures. These nanoparticles showed excellent photocatalytic activity under visible light irradiation. Kostedt *et al.* [101] reported TiO_2-ZnO mixed oxide nanoparticles synthesized by precipitation of zinc nitrate and titanium tetrachloride as precursors. The pH was adjusted to 8.5 by slowly adding an ammonium hydroxide solution and continuing to stir for 2 h. White $Zn(OH)_2/Ti(OH)_4$ precipitate formed instantaneously. Daly *et al.* [102] prepared samples of TiO_2-ZrO_2 using co-precipitation method. The co-precipitated hydroxides were prepared in three ways: by homogenous precipitation of $TiCl_4$ and $ZrOCl_2 \cdot 8H_2O$ with urea, by direct addition of ammonium hydroxide to $TiCl_4$ and $ZrOCl_2 \cdot 8H_2O$ and by hydrolysis of metal alkoxides (titanium(IV) butoxide and zirconium n-propoxide) in n-propanol. The calcination of hydroxides was done

at 300-700ºC. Wu *et al.* [103] prepared TiO$_2$-ZnO mixed oxides from anhydrous alcohol solution containing equal moles of TiCl$_4$ and ZrCl$_4$ by adding 28% aqueous solution of ammonia. In recent years, coating process with nanoparticles through the heterogeneous precipitation method has been widely used for the synthesis of the composite materials [104]. This process improves not only the sintering activity and densification, but also the different phase uniformity and mechanical properties of the sintered body [105,106].
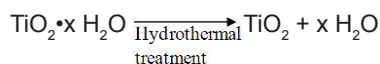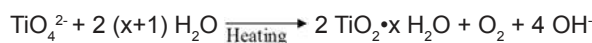
Wang *et al.* [107] prepared TiO$_2$-Al$_2$O$_3$ supports with high specific surface area and large pore diameter using ultrasound-assisted precipitation. Ultrasound could produce the strong chemical and mechanical effects, which was beneficial to inhibit the agglomeration of the nanoparticles. Using anhydrous ethanol to replace the water in the as-prepared support could hinder the particles agglomeration and then increased the specific surface area and the pore diameter significantly. Adding CTAB in the as-prepared support before calcination could enlarge the pore volume greatly. Tyrpekla *et al.* [108] reported magnetically separable photocatalytic active composite γ-Fe$_2$O$_3$@TiO$_2$ synthesized by heterogeneous precipitation. The magnetic carrier (maghemite nanoparticle prepared by a precipitation method and consequently covered by the citric acid in order to adjust the zeta-potential of the particle surface) was enfolded by TiO$_2$ *via* heterogeneous precipitation of TiOSO$_4$ using urea as a precipitation agent. The process of annealing affected crystallinity and phase of the composite and consequently its photocatalytic activity. The procedure was designed to minimize the production cost in order to be easily transferred into the industrial scale while conserving the high quality of the photoactive product.

5. Hydrothermal method

Hydrothermal synthesis involves water both as a catalyst and occasionally as a component of solid phases at elevated temperature (>100°C) and pressure (more than a few bars) [109]. It is an attractive techniques to produce mono-dispersed and highly homogeneous nanoparticles, and to process nano-hybrid and nanocomposite materials [110] widely used in the ceramics industry [111]. Several authors have studied in detail the mild hydrothermal synthesis of TiO$_2$ particles and the influence of various parameters like temperature, experimental duration, pressure (percentage fill), solvent type, pH, and the starting charge on the resultant product. The synthesis of TiO$_2$ is usually carried out in small autoclaves of the Morey type, provided with Teflon liners. The conditions

selected for the synthesis of TiO$_2$ particles are: T ≤ 200ºC, P < 100 bars. The use of Teflon liners helps to obtain pure and homogeneous TiO$_2$ particles. Solutions of NaOH, KOH, HCl, HNO$_3$, HCOOH and H$_2$SO$_4$ were treated as mineralisers and it was found that HNO$_3$ was a better mineraliser for obtaining mono-dispersed nanoparticles of TiO$_2$ with homogeneous composition under the present experimental conditions [112].

Qian *et al.* [113] have reported the preparation of ultrafine powders of TiO$_2$ by hydrothermal H$_2$O$_2$ oxidation starting from metallic Ti. This can be done in two steps: (i) oxidation of Ti with an aqueous solution of H$_2$O$_2$ and ammonia to form a gel (TiO$_2$, H$_2$O); (ii) hydrothermal treatment of gel under various conditions. It is expressed as follows:

$$Ti + H_2O_2 + 2\ OH^- \xrightarrow{\text{Oxidation}} TiO_4^{2-} + 4\ H_2O$$

$$TiO_4^{2-} + 2\ (x+1)\ H_2O \xrightarrow{\text{Heating}} 2\ TiO_2 \cdot x\ H_2O + O_2 + 4\ OH^-$$

$$TiO_2 \cdot x\ H_2O \xrightarrow[\text{treatment}]{\text{Hydrothermal}} TiO_2 + x\ H_2O$$

Hydrothermal method has been found to be very convenient for preparation of TiO$_2$ nanotubes / nanofibers [114-117]. Kim *et al.* [117] prepared sodium titanate nanotubes by the hydrothermal synthesis of Degussa P25 powders at a reaction temperature of 150ºC, 10 M NaOH concentration and reaction time of 48 h. The resulting product did not contain any remnants of Degussa P25 nanoparticles and the resulting nanotubes had a very smooth morphology without the presence of any bundle-like structures. Yan *et al.* [118] reported a facile ethanol induced hydrothermal synthesis of rutile TiO$_2$ nanotubes without the need of molds or templates for replication. The synthesis was carried out in ethanol-water solution using the TiO$_2$ particles with mixed anatase and rutile phase as precursor. The phase transformation from anatase to rutile was promoted through the chelating role of ethanol to the TiO$_6$ octahedra. They found that the water-ethanol ratio and the type of alcohol have important influence on the shape and phase structure of the products. Xu *et al.* [119] prepared single-crystalline TiO$_2$ nanomaterial with controllable phase composition and morphology by hydrothermally treating suspensions of the H-titanate nanotubes at different pH and temperature. During hydrothermal treatment of H-titanate nanotubes dispersed in an acid medium, the nanotubes transformed into tiny anatase nanocrystallites of about 3 nm as an intermediate of peptization. These intermediate nanocrystallites predominantly transformed into anatase nanoparticles with rhombic shape when the pH value was greater than or equal to 1.0, whereas primarily turned into rutile

nanorods with two pyramidal ends at the pH value less than or equal to 0.5 thus forming TiO_2 nanomaterials with controlled phase composition and morphology (Fig. 3). This growth process involves the steps of protonation, oriented attachment, and Ostwald ripening.

Zhao et al. [120] reported the synthesis of mesoporous TiO_2 by hydrothermal method using cetyltrimethyl ammonium bromide (CTAB) as a template. Wang et al. [121] reported that mesoporous TiO_2 synthesized by hydrothermal method exhibited good catalytic activity for degradation of methyl orange. Pavasupree et al. [122] synthesized mesoporous anatase TiO_2 nanopowders by hydrothermal method and these nanopowders showed high activity as compared with nanosized TiO_2 (Degussa P25) on the oxidation photo-reaction of I to I_2 in excess I conditions. Wu et al. [123] synthesized TiO_2 microspheres with extremely uniform sizes of about 2 μm in diameter by alkaline hydrothermal treatment of metallic Ti and hydrogen peroxide and their subsequent proton exchange followed by calcination in air. The microspheres were urchin-like aggregates of radially assembled nanowires, which consisted of chain-like anatase single crystallites with an average diameter of 20–25 nm. The homogeneous microspheres exhibited an excellent activity to assist photodegradation of rhodamine B in water, which is significantly higher than that of P25 TiO_2 nanoparticles. These homogeneous microspheres find practical applications in efficient photocatalytic treatments of dye effluents because of the much easier recovery of the photocatalyst.

Wang et al. [124] reported nanoscale CNTs/P-TiO_2 photocatalyst prepared by hydrothermal method for degradation of methyl orange dye under UV and visible irradiation. CNTs/P-TiO_2 photocatalyst so prepared had a smaller crystalline size, larger surface area and stronger absorption in the visible range than pure TiO_2. The surface states of phosphorus allowed more efficient utilization of both UV and visible-light due to the generation of the Ti–O–P linkage in the photocatalyst and the presence of CNTs promotes the separation of photogenerated carriers. Zhang et al. [125] proposed a green and facile way to synthesize TiO_2/graphene sheet composites from $TiCl_4$ and graphene oxide solution by a one-step hydrothermal method. TiO_2 is chemically bonded to graphene sheet through interaction of titanium ions and the oxygen functionalities in graphene oxide. Significant improvement in the photocatalytic hydrogen evolution was observed for the hydrothermally prepared TiO_2/graphene sheet composite as compared to that of Degussa P25 and the sol-gel obtained TiO_2/graphene sheet composites in their previous work [126].

Zhang et al. [127] employed microwave-assisted hydrothermal method to synthesize nitrogen doped TiO_2 nanoparticles. Due to the high heating efficiency of microwave, rapid synthesis could be achieved as compared to the conventional method. With this approach nitrogen doped TiO_2 could be prepared in extremely short time, even as short as 5 min. The prepared samples showed high specific surface areas, and consisted of mixed phases of anatase, monoclinic and very little rutile phase. Compared with the nitrogen doped TiO_2 synthesized through conventional hydrothermal method, the samples showed even higher photocatalytic activities.

6. Solvothermal method

The solvothermal method is almost identical to the hydrothermal method except that organic solvents are used instead of water [128-130]. This method can be defined as a chemical reaction or transformation in an organic solvent like methanol [131], 1,4 butanol [132], toluene [133] under supercritical pressure and temperature [134]. Generally, a subsequent thermal treatment is required to crystallize the final material. Particle morphology, crystalline phase, and surface chemistry of the solvothermal-derived TiO_2 can be easily controlled by regulating precursor composition, reaction temperature, pressure, solvent property, and aging time [93]. In comparison with the hydrothermal method, the solvothermal method allows the product to be free from foreign anions because the organic solution, having a low relative permittivity, is free from ionic species [134]. Solvothermal processing provides for excellent chemical homogeneity and the possibility of deriving unique metastable structures at low reaction temperatures. The prepared TiO_2 nanoparticles exhibited photocatalytic activity much higher than those of commercial TiO_2 products [135].

Many research groups used solvothermal method for the synthesis of TiO_2. Lee et al. [136] synthesized colloidal solutions containing nanosized TiO_2 particles by employing solvothermal as well as sol-gel method (Fig. 4). A thin film obtained from solvothermal route had smaller and more uniform TiO_2 particles and had the anatase structure even after drying at 200°C. However, a much thinner film could be obtained using sol-gel method that remained stably attached on a silicon wafer or on a Pyrex plate after thermal treatment. Kongsuebchart et al. [137] synthesized nano-TiO_2 powders with average crystallite sizes in the range of 9-15 nm by solvothermal method. The crystallite size of TiO_2 was varied by
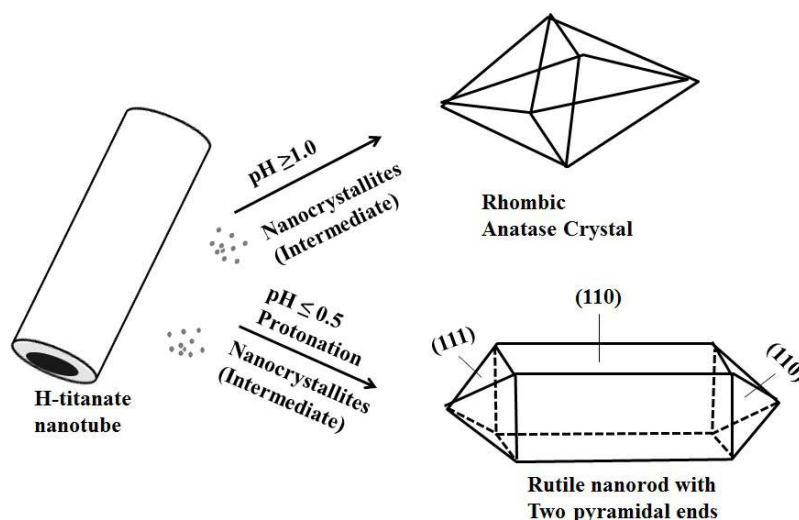
Figure 3. Schematic diagram for the mechanism of hydrothermal transformation from H-titanate nanotubes into single-crystalline TiO$_2$ nanomaterial with different phase composition and morphology [119].

changing the concentrations of titanium(IV) n-butoxide, reaction temperature and the holding time. Increasing reaction temperature and holding time resulted in an increase in the average crystallite size of TiO$_2$. Kaewgun *et al.* [138] prepared polymorphic TiO$_2$ nanoparticles by a water-based ambient condition sol process and post-treated them by a solvent-based ambient condition sol process. The hydroxyl contents in water-based ambient condition sol sample were minimized *via* a solvent-based ambient condition sol process. The synthetic scheme is given in Fig. 5. Evaluation of methyl orange degradation under UV irradiation results showed that the lower lattice hydroxyl content in solvent-based ambient condition sol TiO$_2$ nanoparticles enhanced the photocatalytic activity. As-prepared TiO$_2$ and post-treated solvent-based ambient condition sol samples, which had similar surface areas and crystallinity, were compared in order to prove that the superior photocatalytic activity came from a reduction in lattice hydroxyl content.

Cheng *et al.* [139] introduced a combined sol-gel and solvothermal process to fabricate mono-dispersed TiO$_2$ microspheres with hierarchical structures using lauryl alcohol as structure-directing agent. The molar ratio of lauryl alcohol, water and tetra-n-butyl titanate was the key factor for the formation of the mono-dispersed TiO$_2$ with anatase phase and the optimal ratio was 1.2:4:1. These microspheres exhibited higher photocatalytic efficiency as compared with commercial Degussa P25 investigated by employing Rhodamine B and Methylene blue as the model compounds. Shen *et al.* [140] reported a microemulsion-mediated solvothermal method to synthesize mixed-phase TiO$_2$ nanocrystals with a tunable anatase/rutile ratio. The ratio of anatase to rutile could

be easily tuned by changing the amount of urea which acted as in situ pH adjusting reagent in aqueous phase of the microemulsion. To confirm the photocatalytic effect of mixed-phase, the degradation of Rhodamine B in aqueous solutions and mineralization of total organic carbon was studied. The catalyst containing 47.6% anatase presented the highest photocatalytic activity.

Yin *et al.* [141,142] prepared nitrogen doped TiO$_2$ (TiO$_{2-x}$N$_y$) by solvothermal process. The solvothermal process could realize the phase compositional and morphological control of the anion-doped photocatalysts. Not only rutile, but also anatase and brookite single phase of TiO$_{2-x}$N$_y$ could be prepared [141]. In addition, the TiO$_{2-x}$N$_y$ with fibrous or wool-like morphologies could be prepared using different precipitants [142]. TiO$_{2-x}$N$_y$ powders prepared by Yin *et al.* [143] showed excellent visible-light absorption, thermal stability and photocatalytic activity for nitrogen monoxide destruction under irradiation of both visible and UV light. About 40% and 60% nitrogen monoxide could be continuously removed with the residence time of 1.9 min by the TiO$_{2-x}$N$_y$ photocatalyst under irradiation of visible-light and UV-light, respectively. Das *et al.* [144] synthesized phase pure anatase TiO$_2$ in different nanoforms such as single-crystalline nanorods, nanowires and nanotubes using a solvothermal route and investigated the effects of the different solvents and reaction time on the shape, size, and the optical properties of the nanostructures. Liu *et al.* [145] prepared nitrogen-doped TiO$_2$ nanoparticles consisting of pure anatase, pure rutile and bicrystallites (anatase + rutile and anatase + brookite) in TiCl$_3$-hexamethylene tetramine alcohol solution under solvothermal process. Anatase gradually transferred
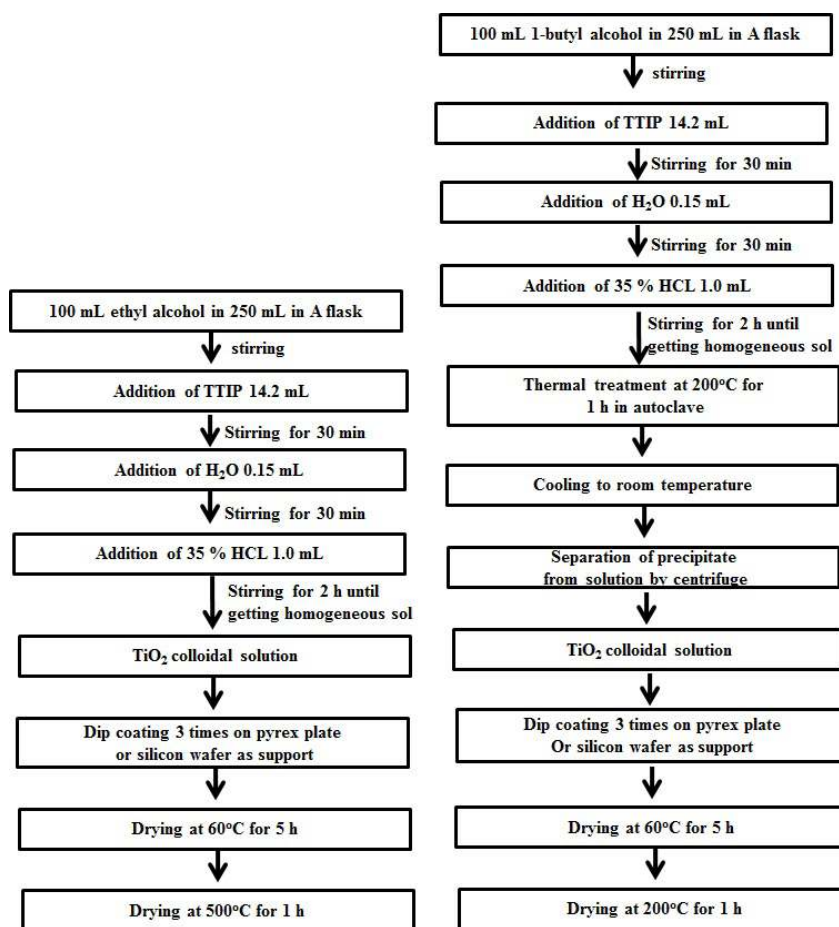
Figure 4. Preparation of TiO$_2$ photocatalyst thin films by (a) sol–gel method and (b) solvothermal method [136].

to rutile with increase of carbon chain using methanol, ethanol, 1-propanol and 1-butanol as solvent. The pure anatase formed at the pH value of 1–2, while bicrystalline TiO$_2$ (anatase + rutile and anatase + brookite) at that of 7–10 in the presence of methanol. The bicrystalline (anatase + brookite) TiO$_2$ demonstrated the best visible photocatalytic activity among all the samples.

7. Electrochemical process

Electrochemical synthesis offers a versatile and low-temperature approach to produce advanced thin films such as epitaxial, superlattice, quantum dot and nanoporous ones. Varying of electrolysis parameters like potential, current density, temperature, and pH can easily control the characteristic states of the films [93].

Both anodic [146,147] and cathodic [148,149] approaches could be utilized for depositing TiO$_2$ although only the anodic electrosynthesis variant appears to have been deployed for applications related to the photoelectrocatalytic (PEC) degradation of organics

[150]. Zwilling and co-workers [151] reported the porous surface of TiO$_2$ films electrochemically formed in fluorinated electrolyte by titanium anodization. Shimizu et al. [152] used dilute sulphuric acid to deposit porous TiO$_2$ thin films at 30°C. Yamamoto et al. [153] found that cathodically electrosynthesized TiO$_2$ films containing occluded commercial Degussa P25 nanoparticles enhanced the performance of dye-sensitized solar cell device.

Patermarakis et al. [154] conducted anodization or anodic oxidation of titanium foils and thin films using a two-electrode electrochemical cell with a platinum foil as cathode at a constant potential and Ti metal as anode. Foils were anodized at different anodizing voltages in 0.5 wt.% HF aqueous solution at room temperature with magnetic agitation of the electrolyte that reduces the thickness of the double layer at the metal/electrolyte interface, and ensures uniform local current density and temperature over the Ti electrode surface.

Grimes and co-workers [155] first reported formation of uniform TiO$_2$ nanotube arrays via anodic oxidation of titanium in a hydrofluoric (HF) electrolyte. Varying pH
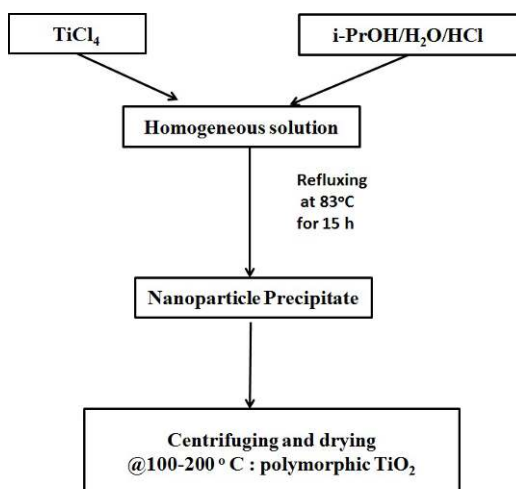
Figure 5. Synthetic diagram for water-based ambient condition sol polymorphic TiO$_2$ [138].

and electrolyte concentration, this same research group produced a 6.4 mm long nanotube array using a fluoride solution of pH 5.5 [156]. Schmuki *et al.* [157,158] also reported the formation of long nanotubes during anodization of titanium in neutral fluoride solutions. The advantage of TiO$_2$ nanotubes produced by anodization or anodic oxidation is that they are readily attached in a perpendicular orientation onto the substrate, which offers much improved electron transfer pathways than non-oriented (random mixtures) structure [159]. Uniform TiO$_2$ nanotube arrays of various pore sizes (22-110 nm), lengths (200-6000 nm), and wall thicknesses (7-34 nm) are easily grown by tailoring electrochemical conditions [160].

Xiao *et al.* [161] reported anatase type TiO$_2$ nanotube arrays fabricated by anodization in dimethyl sulfoxide electrolyte containing 1 wt.% HF solution at above 50°C without subsequently annealing. A two electrode configuration was used for anodization, where the platinum electrode served as cathode. The length of the nanotubes decreases with increasing anodization temperature from about approximately 15 μm at 40°C to approximately 4.5 μm at 60°C. Anatase TiO$_2$ nanotube arrays could be fabricated at 50°C without annealing.

Xie *et al.* [162] fabricated TiO$_2$ nanocomplexes, comprising the disordered nanoribbons or nanowires on the top surface and highly ordered nanotube array on the under-laying layer by longitudinally splitting off nanotubes in a controlled anodization process. The anodization process was carried out in ethylene glycol solution with neutral ammonium fluoride and the controlled water content. Bare titanium sheet was used as an anode and a platinum sheet acted as a cathode. These anatase TiO$_2$ nanocomplexes formed, showed higher photovoltage, photocurrent responses and

photocatalytic activity than TiO$_2$ nanotube array due to the enhanced light harvesting caused by nanoribbons and nanowires.

Ishihara *et al.* [163] prepared nanostructured TiO$_2$ photoanodes by electrochemical anodization of a titanium foil in an electrolyte containing ethylene glycol, ammonium fluoride, and distilled water. The diameters of the nanotubes were varied by adjusting the anodization voltage, and the lengths of the nanotubes were adjusted by varying the time period of anodization. In addition, step-down voltage anodization produced cone-shaped nanotubes with base diameters larger than their tip diameters. The surface of the nanotubular photoanodes was then treated with helium plasma to remove contaminants and reduce the recombination sites. This was followed by nitrogen plasma treatment for surface doping with N$_2$. Surface treatment created oxygen vacancies and induced substitutional doping of N$_2$ at the TiO$_2$ surface. The results showed that the combination of novel surface structures coupled with plasma-assisted surface modification improved the photocurrent density of TiO$_2$ photoanodes.

Zhao *et al.* [164] with an insight towards future implant surface design prepared hierarchical micro/nano-textured surface topographies on titanium by acid etching to produce micropits and subsequent anodization to form a nanotubular layer in order to mimic the hierarchical structure of bone tissues. The sharp edges formed during etching procedure could be smoothed by anodization. This micro-texture induced inconsistent osteoblast functions with initial cell adhesion and osteogenesis-related gene expressions dramatically enhanced while other cell behaviours such as proliferation, intracellular total protein synthesis, alkaline phosphatase activity, extracellular matrix deposition and mineralization are significantly depressed. Nanotubes of different sizes (diameters of about 15 and 80 nm) were distributed quite uniformly on the micro-structured surface. Addition of nanotubes to the micro-structured surface enhanced multiple osteoblast behaviours with nearly all the cell functions retained or promoted.

Wu *et al.* [165] employed micro-arc oxidation process and alkali treatment to develop TiO$_2$ layer with very high specific surface area on pure titanium surface. An anodic dc voltage of 400-500 V was applied in sodium dihydrogen phosphate dehydrate electrolytic solution to titanium plate, followed by alkali treatment to produce nano-flaky anatase TiO$_2$ on surface, with nano-flakes about 50 nm in dimension thus largely increasing the specific surface area. This resulted in significantly increased photovoltaic efficiency when considered using its use as the back electrode of a dye-sensitized solar cell.

Sun *et al.* [166] fabricated highly ordered Fe^{3+}-doped TiO_2 nanotube array films directly by the electrochemical anodic oxidation of pure titanium in an HF electrolyte solution containing iron ions with a platinum counter electrode. The strong enhancement of the photocurrent and the obvious absorption for TiO_2 nanotube arrays are related to the Fe^{3+} dopant. The appropriate amount of doped Fe^{3+} in TiO_2 nanotube array film plays a crucial role in effectively improving its photocatalytic activity under UV-irradiation.

8. Biological synthesis

The interaction between inorganic nanoparticles and biological structures is one of the most exciting areas of research [167]. It is established that many organisms can produce inorganic materials either intra- or extracellularly. The use of microorganism is an eco-friendly approach to prepare nanomaterials under mild conditions that is devoid of using toxic chemicals in the synthesis protocol [168].

Bacteria-derived nanoparticles may show considerable polydispersity because size of the mineral particles is affected by cell growth of the bacteria, composition of the incubation solution, and growth conditions of the minerals, but mono-dispersed products can still be obtained by properly controlling the synthetic parameters (concentration, pH, temperature, *etc.*) [169,170]. Jha *et al.* [168] reported *Lactobacillus sp.* mediated biosynthesis of TiO_2 nanoparticles as green cost-effective biosynthetic method. The average particle sizes were estimated to be of the order of 30 nm.

The bacteria-based synthesis is versatile to produce hollow nanostructures that are expected to display enhanced functions compared with their solid counterparts. Besides, bacteria in a range of morphologies can be utilized to produce hollow nanostructures of other forms besides hollow spheres. For example, bacillus, spirillum, vibrio, fusiform bacteria, square bacteria, star-shaped bacteria, can lead to hollow structures of nanotubes, nanohelixes, nanocables, twin spheres, chain spheres, *etc.* [171]. Kirthi *et al.* [172] synthesized titanium dioxide nanoparticles using bacterium *Bacillus subtilis*. This presented an inexpensive, non-toxic, eco-friendly, fast and reproducible method for the preparation of pure form of nanoparticles using an abundantly available microorganism. The morphological characteristics were found to be spherical, oval in shape, individual nanoparticles as well as a few aggregates having the size of 66-77 nm.

Similar to bacteria, fungi and yeasts are also capable of producing minerals through microbial processes, which inspire novel synthetic routes for metal and semiconductor nanomaterials [171]. Bansal *et al.* [173] used *Fusarium oxysporum* for the production of TiO_2 nanoparticles from aqueous anionic complex TiF_6^{2-}. Extra-cellular protein-mediated hydrolysis of the anionic complexes results in the facile room temperature synthesis of crystalline TiO_2 particles. Jha *et al.* [168] used *Lactobacillus sp.* and baker's Yeast (*S. cerevisiae*) for the synthesis of TiO_2 nanoparticles. TiO_2 might have resulted due to pH-sensitive membrane bound oxido-reductases and carbon source dependent rH_2 in the culture solution. Cui *et al.* [174] synthesized ordered hierarchical mesoporous TiO_2 by using yeast
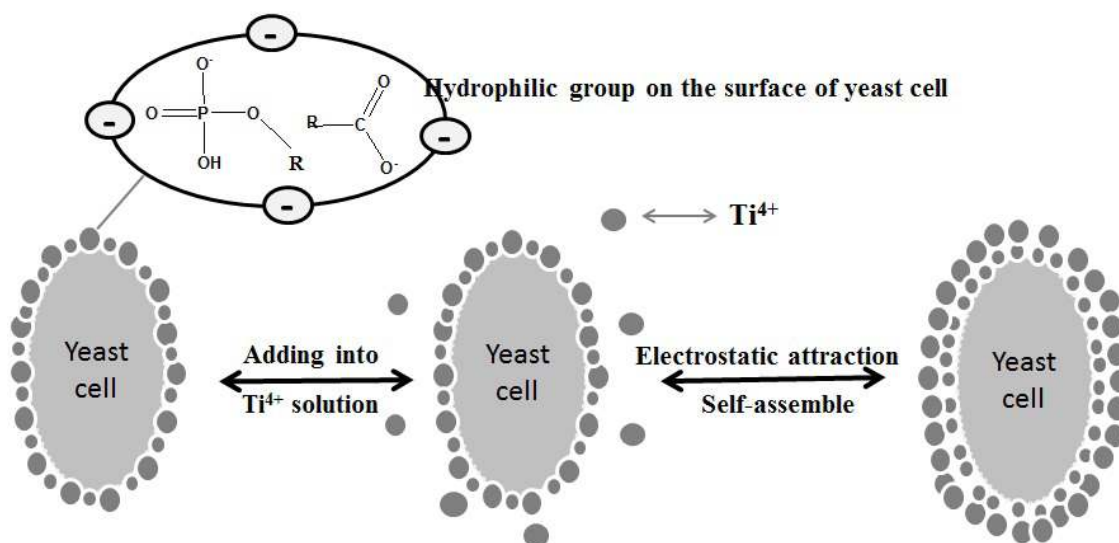

Figure 6. Preparation process of ordered hierarchical mesoporous TiO_2 [174].

cells as the template *via* biomimetic mineralization (Fig. 6). During the cultivation of yeast cells, a bioemulsifier with some hydrophilic anion groups including carboxyl (COO−) and –OPO_3^{2-} were produced on the surface of cells. When $TiCl_4$ solution was mixed with yeast and stirred at room temperature, positively charged titanium cations were combined with the negatively charged COO− and –OPO_3^{2-} groups, and were self-assembled to the yeast cells surface by electrostatic interaction. On addition of ammonia hydroxide to the system, yeast/$Ti(OH)_4$ core-shell spheres were formed due to in situ hydrolysis and condensation of titanium cations. Finally, after calcination, the yeast/$Ti(OH)_4$ core-shell spheres converted to mesoporous TiO_2 and the products retained the profile of the yeast cell walls.

Sundrarajan *et al.* [175] reported an eco-friendly method for the synthesis of TiO_2 nanoparticles from titanium isopropoxide solution using nyctanthes leaves extract. Leaves of nyctanthes arbor-tristis were collected, washed and dried at room temperature, cut into fine pieces, grinded and sieved to get a fine powder. This powder was mixed with ethanol and extracted under reflux condition at 50°C. The ethanolic leaf extract was reacted with titanium tetraisoproxide under stirring at 50°C for four hours to obtain TiO_2 nanoparticles. TiO_2 nanoparticles separated by centrifugation were calcinated at 500°C. The prepared nanoparticles exhibit spherical morphology and particle size in the range of 100-150 nm.

TiO_2 has become one of the most extensively studied non-biological inorganic materials to be synthesized by biomolecules [176-183]. The enzyme lysozyme and several peptides identified through the screening of a phage-displayed peptide library have also been explored for the biomimetic production of TiO_2 [180,181,184,185].

9. Conclusion

Over the past decades, tremendous efforts have been put into TiO_2 nanomaterials, which have resulted in a rich database of their synthesis, properties, modifications and applications. The continuing breakthroughs in the synthesis of TiO_2 nanomaterials have brought new properties and new applications with improved performance. In this review, we have described various solution routes for the synthesis of TiO_2 by sol-gel, microemulsion, precipitation, hydrothermal, solvothermal, electrochemical and biological strategies. Each method has its own importance and advantage. Precipitation is a widely used and simple method. However, one of the limitations of precipitation method is the tedious control of particle size and size distribution, as fast precipitation often causes formation of larger particles instead of nanoparticles. The advantage of the microemulsion route is that the size of the particles can be affected by the ratio of surfactant to water. The advantages of sol-gel processing are ambient temperature of sol preparation and gel processing, high purity of precursors, product homogeneity, low temperature of sintering, ease of making multicomponent materials and good control on powder particle size and shape. Hydrothermal and solvothermal processing provide excellent chemical homogeneity and the possibility of deriving unique metastable structures at low reaction temperatures. In comparison with the hydrothermal method, the solvothermal method allows the product to be free from foreign anions because organic solutions have a low relative permittivity. Electrochemical synthesis offers a versatile and low-temperature approach to produce advanced thin films such as epitaxial, superlattice, quantum dot and nanoporous ones. The use of microorganism is an eco-friendly approach to synthesize nanomaterials under mild conditions that is devoid of using toxic chemicals in the synthesis protocol.

Acknowledgment

References

[1] A. Fujishima, K. Honda, Nat. 238, 37 (1972)

[2] M. Gratzel, Nat. 414, 338 (2001)

[3] A. Hagfeldt, M. Gratzel, Chem. Rev. 95, 49 (1995)

[4] A.L. Linsebigler, G. Lu, J.T.Jr. Yates, Chem. Rev. 95, 735 (1995)

[5] A. Millis, S.J. Le Hunte, J. Photochem. Photobiol. A 108, 1 (1997)

[6] V.K. Gupta, R. Jain, S. Agarwal, M. Shrivastava, Colloids and Surfaces A: Physicochem. Eng. Aspects 378, 22 (2011)

[7] V.K. Gupta, R. Jain, A. Nayak, S. Agarwal, M. Shrivastava, Mater. Sci. and Eng. C 31, 1062 (2011)

[8] G. Pfaff, P. Reynders, Chem. Rev. 99, 1963 (1999)

[9] A. Salvador, M.C. Pascual-Marti, J.R. Adell, A. Requeni, G. March, J. Pharm. Biomed. Anal. 22, 301 (2000)

[10] M.D. Newman, M. Stotland, J.I. Ellis, J. American Acad. Derm. 61, 685 (2009)

[11] R. Zallen, M.P. Moret, Solid State Commun. 137, 154 (2006)

[12] J.H. Braun, A. Baidins, R.E. Marganski, Prog. Org. Coat. 20, 105 (1992)

[13] M.A. Behnajady, H. Eskandarloo, N. Modirshahla, M. Shokri, Desalination 278, 10 (2011)

[14] C. Burda, X. Chen, R. Narayanan, M.A. El-Sayed, Chem. Rev. 105, 1025 (2005)

[15] D. Ganguli, Bull. Mater. Sci. 15, 421 (1992)

[16] Y. Li, T. White, S.H. Lim, Rev. Adv. Mater. Sci. 5, 211 (2003)

[17] G. Colón, M.C. Hidalgo, J.A. Navío, Catal. Today 76, 91 (2002)

[18] N. Uekawa, J. Kajiwara, K. Kakegawa, Y. Sasaki, J. Colloid Interface Sci. 250, 285 (2002)

[19] A.J. Maira, K.L. Yeung, J. Soria, J.M. Coronado, C. Belver, C.Y. Lee, V. Augugliaro, Appl. Catal. B 29, 327 (2001)

[20] B. Li, X. Wang, M. Yan, L. Li, Mater. Chem. Phys.78, 184 (2003)

[21] H. Parala, A. Devi, R. Bhakta, R.A. Fischer, J. Mater. Chem. 12, 1625 (2002)

[22] K.N.P. Kumar, K. Keizer, A.J. Burggraaf, J. Mater. Chem. 3, 917 (1993)

[23] C.-H. Chang, R. Gopalan, Y.S. Lin, J. Membr. Sci. 91, 27 (1994)

[24] U. Trudinger, G. Muller, K.K. Unger, J. Chromatogr. 535, 111 (1990)

[25] S. Matsuda, A. Kato, Appl. Catal. 8, 149 (1983)

[26] P.D.L. Mercera, J.G. Van Ommen, E.B.M. Doesburg, A.J. Burggraaf, J.H. Ross, Appl. Catal. 71, 363 (1991)

[27] M. Schneider, A. Baiker, Catal. Today 35, 339 (1997)

[28] R. Cai, K. Hashimoto, Y. Kubota, A. Fujishima, Chem. Lett. 427 (1992)

[29] S. Sitkiewitz, A. Heller, New J. Chem. 20, 233 (1996)

[30] N.B. Jackson, C.M. Wang, Z. Luo, J. Schwitzgebel, J.G. Ekerdt, J.R. Brock, A. Heller, J. Electrochem. Soc. 138, 3660 (1991)

[31] Y. Paz, Z. Luo, L. Rabenberg, A. Heller, Journal of Mater. Res. 10, 2842 (1995)

[32] T. Watanabe, A. Kitamura, E. Kojima, C. Nakayama, K. Hashimoto, A. Fujishima, In: D. Oilis, H. El-Akabi (Eds.), Photocatalytic Purification and Treatment of Water and Air (Elsevier, New York, 1993) 747

[33] I. Sopyan, S. Murasawa, K. Hashimoto, A. Fujishima, Chem. Lett. 23, 723 (1994)

[34] N. Negishi, T. Iyoda, K. Hashimoto, A. Fujishima, Chem. Lett. 24, 841(1995)

[35] J.L.H. Chau, H.–W. Liu, W. –F. Su, J. Phys. Chem. Sol. 70, 1385 (2009)

[36] V. Loryuenyong, K. Angamnuaysiri, J. Sukcharoenpong, A. Suwannasri, Ceramics Inter. 2011 (In press)

[37] J.C.S. Wu, C.-H. Chen, J. Photochem. Photobio. A: Chem. 163, 509 (2004)

[38] K. Bhattacharyya, S. Varma, A.K. Tripathi, S.R. Bharadwaj, A.K. Tyagi, J. Phys. Chem. C 112, 19102 (2008)

[39] N.Y. Al-Salim, S. Abagshaw, A. Bittar, T. Kemmett, A.J. McQuilla, A.M. Mills, J. Mater. Chem. 10, 2358 (2000)

[40] I-H. Tseng, W-C. Chang, J.C.S. Wu, Appl. Catal. B: Environ. 37, 37 (2003)

[41] I-H. Tseng, J.C.S. Wu, H.-Y. Chou, J. Catal. 221, 432 (2004)

[42] R. Phani, S. Santucci, Mater. Lett. 50, 240 (2001)

[43] J.A. Navío, G. Colón, M. Macías, C. Real, M.I. Litter, Appl. Catal. A: Gen. 177, 111 (1999)

[44] Z.-H. Yuan, J.-H. Jia, L.-D. Zhang, Mater. Chem. Phys. 73, 323 (2002)

[45] R.S. Sonawane, B.B. Kale, M.K. Dongare, Mater. Chem. and Phys. 85, 52 (2004)

[46] J. Wang, S. Una, K.J. Klabunde, Appl. Catal. B: Environ. 48, 151 (2004)

[47] H. Yamashita, M. Harada, J. Misaka, M. Takeuchi, K. Ikeue, M. Anpo, J. Photochem. Photobiol. A: Chem.148, 257 (2002)

[48] R. Arroyo, G. Córdoba, J. Padilla, V.H. Lara, Mater. Lett. 54, 397 (2002)

[49] T. López, R. Gómez, G. Pecci, P. Reyes, X. Bokhimi, O. Novaro, Mater. Lett. 40, 59 (1999)

[50] A.D. Paola, E. García-López, S. Ikeda, G. Marcì, B. Ohtani, L. Palmisano, Catal. Today 75, 87 (2002)

[51] J. Yu, J.C. Yu, B. Cheng, X. Zhao, J. Sol-Gel Sci. and Tech. 24, 39 (2002)

[52] F.B. Li, X.Z. Li, Appl. Catal. A: Gen. 228, 15 (2002)

[53] N.B. Narayanan, Y. Zahira, R. Ramakrishnan, Cent. Eur. J. Chem. 8, 182 (2009)

[54] F.B. Li, X.Z. Li, M.F. Hou, Appl. Catal. B: Environ. 48, 185 (2004)

[55] H.E. Chao, Y.U. Yun, H.U. Xingfang, A. Larbot, J. Eur. Ceram. Soc. 23, 1457 (2003)

[56] M. Stir, T. Traykova, R. Nicula, E. Burkel, C. Baehtz, M. Knapp, C. Lathe, Nucl. Instrum. Meth. Phys. Res. B 199, 59 (2003)

[57] P. Yang, C. Lu, N. Hua, Y. Du, Mater. Lett. 57, 794

(2002)

[58] C. Wang, C. Bottcher, D.W. Bahnemann, J.K. Dohrmann, J. Mater. Chem. 13, 2322 (2003)

[59] R. Subasri, M. Tripathi, K. Murugan, J. Revathi, G.V.N. Rao, T.N. Rao, Mater. Chem. Phys. 124, 63 (2010)

[60] J. Wang, W. Zhu, Y. Zhang, S. Liu, J. Phys. Chem. C 111, 1010 (2007)

[61] C.-C Pan, J.C.S. Wu, Mater. Chem. Phys. 100, 102 (2006)

[62] S.C. Moon, H. Mametsuka, E. Suzuki, Y. Nakahara, Catal. Today 45, 79 (1998)

[63] X. Song, L. Gao, J. Phys. Chem. C 111, 8180 (2007)

[64] P.D. Cozzoli, E. Fanizza, M.L. Curri, D. Laub, A. Agostiano, Chem. Commun. 942 (2005)

[65] P.D. Cozzoli, A. Kornowski, H. Weller, J. Am. Chem. Soc. 125, 14539 (2003)

[66] P.D. Cozzoli, E. Fanizza, R. Comparelli, M. L. Curri, A. Agostiano, D. Laub, J. Phys. Chem. B 108, 9623 (2004)

[67] P.D. Cozzoli, R. Comparelli, E. Fanizza, M. L. Curri, A. Agostiano, D. Laub, J. Am. Chem. Soc. 126, 3868 (2004)

[68] P.D. Cozzoli, M.L. Curri, A. Agostiano, Chem. Commun. 3186 (2005)

[69] N.S. Venkataramanan, K. Matsui, H. Kawanami, Y. Ikushima, Green Chem. 9, 18 (2007)

[70] S. Liu, J. He, J. Am. Ceram. Soc. 88, 3513 (2005)

[71] Y. Gu, X. Liu, T. Niu, J. Huang, Mater. Research Bulletin 45, 536 (2010)

[72] D. Zhang, L. Qi, Chem. Commun. 21, 2735 (2005)

[73] V. Chhabra, V. Pillai, B.K. Mishra, A. Morrone, D.O. Shah, Langmuir 11, 3307 (1995)

[74] R. Leung, M.J. Hou, D.O. Shah, In: D.T. Wasan, M.E. Ginn, D.O. Shah (Eds.), Surfactant Sci. Series Vol. 28 (Marcel Dekker, New York, 1988) 315.

[75] H. Gutmann, A.S. Kertes, J. Colloid Interface Sci. 51, 406 (1973)

[76] P. Pieranski, Phys. Rev. Lett. 45, 569 (1980)

[77] O.D. Velev, K. Furusawa, K. Nagayama, Langmuir 12, 2374 (1996)

[78] M. Andersson, L. Österlund, S. Ljungström, A. Palmqvist, J. Phys. Chem. B 106, 10674 (2002)

[79] M.P. Pileni, Langmuir 13, 3266 (1997)

[80] R. Zhang, L. Gao, Mater. Res. Bull. 37, 1659 (2002)

[81] K.T. Lim, H.S. Hwang, W. Ryoo, K.P. Johnson, Langmuir 20, 2466 (2004)

[82] V. Pillai, P. Kumar, M.J. Huo, P. Ayyub, D.O. Shah, Adv. Colloid Interface Sci. 55, 241 (1995)

[83] K. Kandori, K. Konno, A. Kitahara, J. Colloid Interface Sci. 122, 78 (1988)

[84] V. Chhabra, P. Ayyub, S. Chattopadhay, A.N. Maitra, Mater. Lett. 26, 21 (1996)

[85] F.A. Deorsola, D. Vallauri, Powd. Tech. 190, 304 (2009)

[86] M. Wu, J. Long, A. Huang, Y. Luo, Langmuir 15, 8822 (1999)

[87] X. Gao, J. Li, W. Gao, Coll. Journal 70, 392 (2008)

[88] C.E. Zubieta, J.F.A.S. Martínez, C.V. Luengo, P.C. Schulz, Powd. Tech. 212, 410 (2011)

[89] Y. Cong, L. Xiao, J. Zhang, F. Chen, M. Anpo, Res. Chem. Intermed. 32, 717 (2006)

[90] C. Adán, A. Bahamonde, M. Fernández-García, A. Martínez-Arias, App. Catal. B, 72, 11 (2007)

[91] A. Zielińska, E. Kowalska, J.W. Sobczak, I. Łącka, M. Gazda, B. Ohtani, J. Hupka, A. Zaleska, Sep. Purif. Tech. 72, 309 (2010)

[92] J.A. Schwarz, Chem. Rev. 95, 477 (1995)

[93] O. Carp, C.L. Huisman, A. Reller, Prog. in Solid State Chem. 32, 33 (2004)

[94] S.C. Davis, K.J. Klabunde, Chem. Rev. 82, 153 (1982)

[95] S. Cheng, S.-Y. Cheng, J. Catal. 122, 1 (1990)

[96] H.E. Namin, H. Hashemipour, M. Ranjbar, Inter. J. Mod. Phys. B 22, 3210 (2008)

[97] Y. Shchipunova, I. Postnova, Coll. Surf. B: Biointer. 74, 172 (2009)

[98] X. You, F. Chen, J. Zhang, M. Anpo, Catal. Lett. 102, 3 (2005)

[99] J.-M. Wu, B. Qi, J. Phys. Chem. C 111, 666 (2007)

[100] T. Sato, Y. Aita, M. Komatsu, S. Yin, J. Mater. Sci. 41, 1433 (2006)

[101] W.L. Kostedt, A.A. Ismail, D.W. Mazyck, Ind. Eng. Chem. Res. 47, 1483 (2008)

[102] F.P. Daly, H. Ando, J.L. Schmitt, E.A. Sturm, J. Catal. 108, 401 (1987)

[103] J.-C. Wu, C.-S. Chung, C.-L. Ay, I. Wang, J. Catal. 87, 98 (1984)

[104] W.J. Tuan, H.H. Wu, T.J. Yang, J. Mater. Sci. 30, 855 (1995)

[105] P.-H. Xiang, X.-L. Dong, C.-D. Feng, Y.-L. Wang, J. Am. Ceram. Soc. 86, 1631 (2003)

[106] P.-H. Xiang, N. Zhong, X.-L. Dong, R.-H. Liang, H. Yang, C.-D. Feng, Mater. Lett. 58, 2675 (2004)

[107] W. Wang, Y. Yang, H. Luo, T. Hu, F. Wang, W. Liu, J. Alloys Comp. 509, 3430 (2011)

[108] V. Tyrpekla, J.P. Vejpravova, A.G. Roca, N. Murafa, L. Szatmary, D. Niznansky, Appl. Surf. Sci. 257, 4844 (2011)

[109] S. Sōmiya, R. Roy, Bull. Mater. Sci. 23, 453 (2000)

[110] K. Byrappa, T. Adschiri, Prog. Crys. Growth

Charac. Mater. 53, 117 (2007)

[111] X. Chen, S.S. Mao, Chem. Rev. 107, 2891 (2007)

[112] K. Byrappa, K.M. Lokanatha Rai, M. Yoshimura, Env. Tech. 21, 1085 (2000)

[113] Y. Qian, Q. Chen, Z. Chen, C. Fan, G. Zhou, J. Mater. Chem. 3, 203 (1993)

[114] D.S. Seo, J.M. Lee, H. Kim, J. Cryst. Growth 229, 428 (2001)

[115] T. Kasuga, M. Hiramatsu, A. Hoson, T. Sekino, K. Niihara, Langmuir 14, 3160 (1998)

[116] X.M. Sun, Y.D. Li, Chem. Eur. J. 9, 2229 (2003)

[117] G.-S. Kim, Y.-S. Kim, H.-K. Seo, H.-S. Shin, Korean J. Chem. Eng. 23, 1037 (2006)

[118] J. Yan, S. Feng, H. Lu, J. Wang, J. Zheng, J. Zhao, L. Li, Z. Zhu, Mater. Sci. and Engineering B 172, 114 (2010)

[119] Y. Xu, X. Fang, J. Xiong, Z. Zhang, Mater. Research Bulletin 45, 799 (2010)

[120] Q. Zhao, J. Chu, T. Jiang, H. Yin, Korean J. Chem. Eng. 25, 1008 (2008)

[121] Z. Wang, T. Jiang, Y. Du, K. Chen, H. Yin, Mater. Lett. 60, 2493 (2006)

[122] S. Pavasupree, J. Jitputti, S. Ngamsinlapasathian, S. Yoshikawa, Mater. Res. Bulletin 43, 149 (2008)

[123] J.–M. Wu, X.–M. Song, M. Yan, J. Hazard. Mater. 194, 338 (2011)

[124] S. Wang, S. Zhou, J. Hazard. Mater. 185, 77 (2011)

[125] X. Zhang, Y. Sun, X. Cui, Z. Jiang, Inter. J. Hyd. Ener. (in press)

[126] X.Y. Zhang, H.P. Li, X.L. Cui, Y. Lin, J. Mater. Chem. 20, 2801 (2010)

[127] P. Zhang, B. Liu, S. Yin, Y. Wang, V. Petrykin, M. Kakihana, T. Sato, Mater. Chem. Phys. 116, 269 (2009)

[128] Y. Qian, Advced Mat. 11, 1101 (1999)

[129] C. Wang, Z.-X. Deng, Y. Li, Inorg. Chem. 40, 5210 (2001)

[130] Z. Zhu, L.Y. Tsung, M. Tomkiewicz, J. Phys. Chem. 99, 15945 (1995)

[131] S. Yin, Y. Fujishiro, J. Wu, M. Aki, T. Sato, J. Mater. Processing Tech. 137, 45 (2003)

[132] M. Kang, J. Mol. Catal. A: Chem. 197, 173 (2003)

[133] C.-S. Kim, B.K. Moon, J.-H. Park, S.T. Chung, S.-M. Son, J. Cryst. Growth 254, 405 (2003)

[134] D. Chen, R. Xu, J. Mater. Chem. 8, 965 (1998)

[135] W.S. Nam, G.Y. Han, Korean J. Chem. Eng. 20, 1149 (2003)

[136] S.-H. Lee, M. Kang, S.M. Cho, G.Y. Han, B.-W. Kim, K.J. Yoon, C.-H. Chung, J. Photochem. Photobiol. A: Chem. 146, 121 (2001)

[137] W. Kongsuebchart, P. Praserthdam, J. Panpranot, A. Sirisuk, P. Supphasrirongjaroen,

C. Satayaprasert J. Crys. Growth 297, 234 (2006)

[138] S. Kaewgun, C.A. Nolph, B.I. Lee, L.–Q. Wang, Mater. Chem. Phys. 114, 439 (2009)

[139] Q.-Q. Cheng, Y. Cao, L. Yang , P.–P. Zhang, K. Wang, H.–J. Wang, Mater. Research Bulletin 46, 372 (2011)

[140] X. Shen, J. Zhang, B. Tian, J. Hazard. Mater. 192, 651 (2011)

[141] S. Yin, Y. Aita, M. Komatsu, J. Wang, Q. Tang, T. Sato, J. Mater. Chem. 15, 674 (2005)

[142] S. Yin, K. Ihara, Y. Aita, M. Komatsu, T. Sato, J. Photochem. Photobiol. A 179, 105 (2006)

[143] S. Yin, M. Komatsu, B. Liu, R. Li, Y. Wang, T. Sato, J. Mater. Sci. 43, 2240 (2006)

[144] K. Das, S.K. Panda, S. Chaudhuri, J. Crystal Growth 310, 3792 (2008)

[145] J. Liu, W. Qin, S. Zuo, Y. Yu, Z. Hao, J. Hazard. Mater. 163, 273 (2009)

[146] N.R. de Tacconi, C.R. Chenthmarakshan, G. Yogeeswaran, A. Watcherenwong, R.S. de Zoysa, N.A. Basit, K. Rajeshwar, J. Phys. Chem. B 110, 25347 (2006)

[147] C.A. Grimes, O.K. Varghese, S. Ranjan, Light, Water, Hydrogen: the solar generation of hydrogen by water photoelectrolysis (Springer, New York, 2008)

[148] G.H.A. Therese, P.V. Kamath, Chem. Mater. 12, 1195 (2000)

[149] C. Natarajan, G. Nogami, J. Electrochem. Soc. 143, 1547 (2006)

[150] K. Rajeshwar, M.E. Osugi, W. Chanmanee, C.R. Chenthamarakshan, M.V.B. Zanoni, P. Kajitvichyanukul, R. Krishnan-Ayer, J. Photochem. Photobiol. C: Photochem. Reviews 9, 171 (2008)

[151] V. Zwilling, M. Aucouturier, E. Darque-Ceretti, Electrochim. Acta 45, 921 (1991)

[152] Y. Shimizu, N. Kuwano, T. Hyodo, M. Egashira, Sens. Actuat. B 83, 195 (2002)

[153] J. Yamamoto, A. Tan, R. Shiratsuchi, S. Hayase, C.R. Chenthamarakshan, K. Rajeshwar, Adv. Mater.15, 1823 (2003)

[154] G. Patermarakis, K. Moussoutzanis, J. Electrochem. Soc. 142, 737 (1995)

[155] D. Gong, C.A. Grimes, O.K. Varghese, W. Hu, R.S. Singh, Z. Chen, E.C. Dickey, J. Mater. Res. 16, 3331 (2001)

[156] Q. Cai, M. Paulose, O.K. Varghese, C.A. Grimes, J. Mater. Res. 20, 230 (2005)

[157] J.M. Macák, H. Tsuchiya, P. Schmuki, Angew. Chem. Int. Ed. 44, 2100 (2005)

[158] M. Macak, H. Tsuchiya, L. Taveira,

S. Aldabergerova, P. Schmuki, Angew. Chem. Int. Ed. 44, 7463 (2005)

[159] P. Xiao, D. Liu, B.B. Garcia, S. Sepehri, Y. Zhang, G. Cao, Sens. Actuators B 134, 367 (2008)

[160] G.K. Mor, O.K. Varghese, M. Paulose, K. Shankar, C.A. Grimes, Sol. Energy Mater. & Solar Cells 90, 2011 (2006)

[161] X. Xiao, K. Ouyang, R. Liu , J. Liang, Appl. Surf. Sci. 255, 3659 (2009)

[162] Y. Xie, D. Fu, Mater. Research Bulletin 45, 628 (2010)

[163] H. Ishihara, J.P. Bock, R. Sharma, F. Hardcastle, G.K. Kannarpady, M.K. Mazumder, A.S. Biris, Chem. Phys. Lett. 489, 81 (2010)

[164] L. Zhao, S. Mei, P.K. Chu, Y. Zhang, Z. Wu, Biomater. 31, 5072 (2010)

[165] S.-Y. Wu, W. -C. Lo, K.-C. Chen, J. -L. He, Curr. App. Phys. 10, S180 (2010)

[166] L. Sun, J. Li , C.L. Wang, S.F. Li, H.B. Chen, C.J. Lin, Sol. Ener. Mater. & Solar Cells 93, 1875 (2009)

[167] A.K. Jha, K. Prasad, A.R. Kulkarni, Int. J. Nanopart. (in press)

[168] A.K. Jha, K. Prasad, A. R. Kulkarni, Coll. and Surfaces B: Biointerfaces 71, 226 (2009)

[169] A. Ahmad, S. Senapati, M.I. Khan, R. Kumar, R. Ramani, V. Srinivas, Nanotech. 14, 824 (2003)

[170] A. Ahmad, S. Senapati, M.I. Khan, R. Kumar, M. Sastry, Langmuir 19, 3550 (2003)

[171] T.-X. Fan, S.-K. Chow, D. Zhang, Progress in Mater. Sci. 54, 542 (2009)

[172] A.V. Kirthi, A.A. Rahuman, G. Rajakumar, S. Marimuthu, T. Santhoshkumar, C. Jayaseelan, G. Elango, A. Abduz Zahir, C. Kamaraj, A. Bagavan, Mater. Letters 65, 2745 (2011)

[173] V. Bansal, D. Rautaray, A. Bharde, K. Ahire, A. Sanyal, A. Ahmad, M. Sastry, J. Mater. Chem. 15, 2583 (2005)

[174] J. Cui, W. He, H. Liu, S. Liao, Y. Yue, Coll. and Surfaces B: Biointerfaces 74, 274 (2009)

[175] M. Sundrarajan, S. Gowri, Chalcogenide Lett. 8, 447 (2011)

[176] J.L. Sumerel, W. Yang, D. Kisailus, J.C. Weaver, J.H. Choi, D.E. Morse, Chem. Mater. 15, 4804 (2003)

[177] N. Kröger, M.B. Dickerson, G. Ahmad, Y. Cai, M.S. Haluska, K.H. Sandhage, N. Poulsen, V.C. Sheppard, Angew. Chem. Int. Ed. 45, 7239 (2006)

[178] M.N. Tahir, P. Théato, W.E.G. Müller, H.C. Schröder, A. Borejko, S. Faiß, A. Janshoff, J. Huth, W. Tremel, Chem. Commun. 5533 (2005)

[179] K.E. Cole, A.N. Ortiz, M.A. Schoonen, A.M. Valentine, Chem. Mater.18, 4592 (2006)

[180] H.R. Luckarift, M.B. Dickerson, K.H. Sandhage, J.C. Spain, Small 2, 640 (2006)

[181] M.B. Dickerson, S.E. Jones, Y. Cai, G. Ahmad, R.R. Naik, N. Kröger, K.H. Sandhage, Chem. Mater. 20, 1578 (2008)

[182] A.M. Azad, S.A. Akbar, S.G. Mhaisalkar, L.D. Birkefeld, K.S. Goto, J. Electrochem. Soc. 139, 3690 (1992)

[183] S.L. Sewell, D.W. Wright, Chem. Mater. 18, 3108 (2006)

[184] K.I. Sano, K.J. Shiba, J. Am. Chem. Soc. 125, 14234 (2003)

[185] K.E. Cole, A.M. Valentine, Biomacromolecules 8, 1641 (2007)